An Eddy-Current Testing Method for Measuring the Thickness of Metallic Plates

Alessandro Sardellitti, *Graduate Student Member, IEEE*, Filippo Milano, *Member, IEEE*, Marco Laracca, *Member, IEEE*, Salvatore Ventre, *Senior Member, IEEE*, Luigi Ferrigno, *Senior Member, IEEE*, and Antonello Tamburrino, *Senior Member, IEEE*

***Abstract*— Thickness measurements of metallic plates are mandatory in many industrial scenarios. Methods based on eddy-current testing (ECT) are ideal for fast and accurate online contactless thickness measurements, making them very attractive in the Industry 4.0 scenario. This contribution is focused on a specific and robust ECT technique proposed in the past by the scientific community. The main limitation is its applicability to thin materials only, where the thickness of the material is much smaller than the overall size of the ECT probe. Extending the range of applicability to thicker materials introduces a progressive and severe degradation of the measurement accuracy. In this article, we analyze the theoretical foundation of this method with an entirely original approach based on the celebrated Buckingham π theorem. In doing this, we draw the complete theoretical picture of the method, providing a simple, clear, and rigorous view of its performance and intrinsic limitations. Moreover, we propose two solutions, one analytical and the other iterative, to accurately estimate the thickness of the materials from thin to thick values. Finally, a numerical analysis combined with an experimental campaign confirms the effectiveness of the proposed solutions, making the method suitable for industrial and other applications.**

***Index Terms*— Eddy-current testing (ECT), nondestructive evaluation (NDE), nondestructive testing (NDT), optimization algorithm, thickness measurement.**

I. Introduction

ACCURATE, low-cost, online, and real-time thickness monitoring of metallic structures is a key issue in many production and diagnostic applications. With regard to the production perspective, the need for accurate online and real-time thickness monitoring is a well-known issue since the final thickness may be different from the expected one, as in the case of welding or mechanical processing. This difference makes it possible to assess the quality of the process and the durability of the material. As for the diagnostic applications, in many practical situations, it is important to evaluate the effects of aging due to environmental and operating conditions, especially when the metallic structures are involved in safety features or are adopted in critical applications. In these contexts, thickness measurements are employed to forecast operating safety for future use and can guide modern diagnostics and predictive maintenance processes, thereby minimizing critical and/or catastrophic failures and related economic and social impacts. In all these applications, the availability of accurate online and real-time monitoring is key for ensuring the timeliness of actions.

Industrial thickness measurement for quality control is commonly viewed as a well-assessed problem, thanks to the availability on the market of accurate measurement instruments based on such technologies as ultrasound [1], lasers [2], and mechanical and touching probes [3]. All these technologies present drawbacks that prevent their use in distributed low-cost, online, and real-time monitoring. For example, solutions based on touching probes are very accurate but require long measurement times. Those based on laser devices call for very high costs, whereas ultrasound technologies require coupling materials whose cleaning increases time and costs. All these drawbacks limit the widespread use of these measurement technologies in modern industrial scenarios where time and cost impose dramatic constraints [4].

Thus, despite the availability of several highly accurate measuring instruments based on the aforementioned technologies, the search for new, accurate, fast, cheap, distributed, online, and real-time measurement methods, technologies, and instruments remains an open issue that is being addressed by numerous researchers around the world [5], [6]. In this framework, several research groups are investigating the possibility offered by eddy-current testing (ECT) techniques [7], which typically assure low costs, simple probes, and ease of realization for online, real-time, and distributed measurement systems.

Several ECT techniques for measuring the thickness of the metallic plates can be found in the literature, most of which rely on multifrequency (MF) and pulsed eddy-current (PEC) methods.

Manuscript received 30 January 2023; revised 25 March 2023; accepted 8 April 2023. Date of publication 24 April 2023; date of current version 10 May 2023. The work was supported by "PiattafoRma Integrata per la Manutenzione e gestione Energetica nella fabbrica intelligente, PRIME" project n. F/190092/03/X44 within Fondo per la Crescita Sostenibile - Sportello "Fabbrica Intelligente" PON I E C 2014-2020 (Prog n. F/190092/03/X44 – CUP:B36G20001160005 COR:3833298) funded by the Italian Ministry of Enterprises and Made in Italy (MISE). The Associate Editor coordinating the review process was Dr. Liuyang Zhang. *(Corresponding author: Filippo Milano.)*

Alessandro Sardellitti, Filippo Milano, and Salvatore Ventre are with the Department of Electrical and Information Engineering, University of Cassino and Southern Lazio, 03043 Cassino, Italy (e-mail: alessandro.sardellitti@unicas.it; filippo.milano@unicas.it; salvatore.ventre@unicas.it).

Marco Laracca is with the Department of Astronautics, Electrical and Energy Engineering, Sapienza University of Rome, 00185 Rome, Italy (e-mail: marco.laracca@uniroma1.it).

Luigi Ferrigno is with the Department of Electrical and Information Engineering, University of Cassino and Southern Lazio, 03043 Cassino, Italy, and also with the Consorzio Nazionale Interuniversitario per le Telecomunicazioni (CNIT), 43124 Pisa, Italy (e-mail: luigi.ferrigno@unicas.it).

Antonello Tamburrino is with the Department of Electrical and Information Engineering, University of Cassino and Southern Lazio, 03043 Cassino, Italy, and also with the Department of Electrical and Computer Engineering, Michigan State University, East Lansing, MI 48824 USA (e-mail: antonello.tamburrino@unicas.it).

Digital Object Identifier 10.1109/TIM.2023.3269781

Within the framework of MF methods, the plate thickness has been estimated by measuring the phase of the complex inductance [8] or through phase analysis of the normalized impedance [9]. Other methods have processed the amplitude of the resistive component of the normalized impedance as a function of the frequency [10]. In this setting, improvements have been achieved in measurement times [11] and robustness to liftoff variations [12], [13].

Regarding the PEC, several studies have proposed the estimation of the thicknesses of conductive samples with proper accuracy and robustness to liftoff variations [14], [15], [16], [17]. Moreover, in [18], MF or PEC are combined for thickness estimation through high-precision measurement using a genetic algorithm-based approach.

The method proposed in this contribution is rooted in the work by Yin and Peyton [10], where they proposed an MF method for thickness measurement of nonmagnetic metallic plates, yielding an accuracy compatible with industrial production standards [19]. The method in [10] is highly efficient, but it relies on the constancy of a certain parameter (α_0 in [10]). Unfortunately, as discussed in Section III, this parameter is highly dependent on the thickness of the specimen, and it can be maintained constantly only asymptotically for thicknesses much smaller than the size of the probe. This makes the method impractical for thick specimens or in the presence of curved surfaces. For instance, in the latter case, there are two conflicting constraints: 1) the probe has to be much larger than the thickness of the specimen and 2) the probe has to be much smaller than the curvature of the specimen, to approximate the surface of the specimen by means of its tangent plane, in a neighborhood of the probe itself.

The aim of this article is to provide a deep, complete, and more general theoretical framework for the method proposed in [10], allowing it to be extended to a broader class of thickness measurements. From the technical perspective, we prove that the critical constant parameter α_0 has to be replaced by a new function $\alpha = \alpha(\Delta)$, which depends on the thickness Δ. With this "minimal" modification, we extend the method's range of applicability while identifying its underlying physical limits.

Moreover, the properties of the new function $\alpha(\cdot)$ are efficiently studied through an entirely original approach based on the celebrated Buckingham π theorem, applied for the very first time in the framework of nondestructive testing.

In addition to the study of theoretical fundamentals, we propose two different algorithms for performing thickness measurement. The first algorithm is iterative and is conceived for applications where the unknown thickness ranges from 0 up to the theoretical limit of the method. This approach requires the knowledge of the function $\alpha(\cdot)$, for a given probe. The second algorithm is based on a polynomial approximation of $\alpha(\cdot)$ and provides the thickness as the solution of an algebraic equation of the same degree as the approximating polynomial. Computationally, this is extremely efficient when the polynomial approximation is up to the third order since the related algebraic equation can be quickly solved in closed form. A higher computational cost is required when increasing the degree of the polynomial approximation.

The resulting measurement method is very efficient in terms of measurement and computational times, and suitable for low-cost measurement architectures, thus ensuring the possibility to get online and real-time measurement instruments for industrial needs.

The article is organized as follows. A short description of the method proposed in [10] is presented in Section II. Then, in Section III, the theoretical foundation of the proposed approach is provided. In this section, we give the fundamental thickness equation (FTE), replacing that given in [10]. The FTE is exact, rather than being valid only in the limit of "small" thicknesses, and the results of [10] can be derived as the limit of the FTE when the thickness approaches 0. Moreover, an in-depth analysis of the structure of the FTE and the global behavior of function $\alpha(\cdot)$ is provided. In Section IV, the intrinsic physical limit of the method is derived. Specifically, it is proved that, for a given probe, the thickness can be estimated (existence, uniqueness, and stability of the solution) up to a certain *Critical Thickness* Δ_c. In Section V, the proposed iterative and analytical approaches to estimate the thickness by solving the FTE are described. The experimental setup and case studies are described in Section VI, whereas the related experimental results are presented and discussed in Section VII. Finally, conclusions are given in Section VIII.

II. Theoretical Framework of Thickness Estimation Using ECT

The ECT principle is based on the interaction between a time-varying magnetic flux density and a conducting material. By supplying an alternating current to an excitation coil, eddy currents are induced in the plate being tested, which generates a reaction magnetic flux density. This reaction field can be measured through the same excitation coil or a different sensing coil or a field sensor. The reaction field depends on the characteristics of the tested material [7]. ECT techniques can be used to measure specimen's electromagnetic properties (electrical conductivity and magnetic permeability, if any) [5], [20], to detect superficial or subsuperficial defects [21], [22], [23], and to measure the thickness of the metallic plates [8], [9], [10], [11], [12], [13], [14], [15], [16], [17], [18].

In this work, we focus on the method proposed by Yin and Peyton [10] aiming to estimate the thickness of a conducting plate by measuring the mutual impedance for a probe comprised of two coils at different frequencies.

Specifically, the key quantity is the variation in the resistance of the mutual impedance ΔR, normalized to the angular frequency ω

$$\frac{\Delta R(\omega)}{\omega} = -\operatorname{Re}\left\{\frac{\dot{Z}_m^P(\omega) - \dot{Z}_m^A(\omega)}{\omega}\right\} \tag{1}$$

where $\dot{Z}_m^P(\omega)$ is the mutual impedance measured on the plate and $\dot{Z}_m^A(\omega)$ is the mutual impedance measured in the air.

According to [10], the thickness Δ of the plate is related to the angular frequency $\omega_{\min}$, where $\Delta R(\omega)/\omega$ achieves its

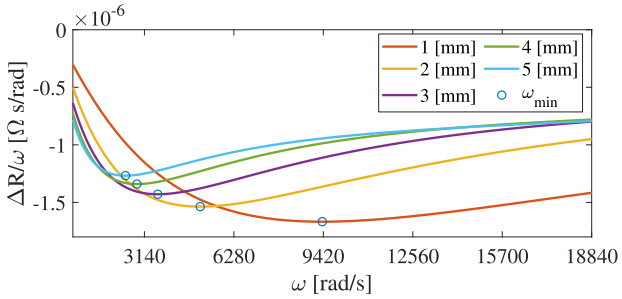

Fig. 1. $\Delta R/\omega$ ratio as a function of ω. Here, $\sigma = 18.8$ MS/m, and the probe is described in Section VI.

minimum value as follows:

$$\Delta = \frac{2\alpha_0}{\sigma \mu_0 \omega_{\min}} \tag{2}$$

where σ is the electrical conductivity of the plate, μ_0 is the free-space magnetic permeability, and, as stated by [10], α_0 is a proper constant related to the geometry of the probe, liftoff, and tilting.

For example, Fig. 1 shows how the $\Delta R(\omega)/\omega$ ratio achieves a minimum, as a function of the angular frequency ω. As expected from (2), $\omega_{\min}$ decreases with the thickness Δ.

III. Fundamental Thickness Equation

Equation (2) is obtained by means of a stationary-phase approach applied to the analytical solution for the eddy-current problem in a plate (see [10]), via the celebrated Dodd and Deeds approach [24]. This approximation is valid as long as

$$\alpha_0 \Delta \ll 1 \tag{3}$$

a condition that is met when the probe coil diameter is much larger than Δ, as stated in [10]. This condition makes it necessary to change the size of the probe when measuring plates of different thicknesses. Moreover, it is an issue when measuring the thickness of the thick plates. This requires a large coil, resulting in encumbrance and other problems.

To overcome the intrinsic limits of (2), here, we derive a new thickness estimation equation, the FTE, with a completely new and original approach based on the celebrated Buckingham π theorem, which is applied for the very first time in the framework of Nondestructive Testing. This new relationship, the FTE, considers all the relevant physics without any approximation, overcoming all the limits of the former. It only requires the knowledge of a function that can be easily evaluated once and for all through numerical simulations or experimental measurements.

Hereafter, we define $\delta_{\min}$ as the skin depth in the conducting material evaluated at the angular frequency $\omega_{\min}$

$$\delta_{\min} = \sqrt{\frac{2}{\sigma \mu_0 \omega_{\min}}}. \tag{4}$$

We have the following theorems, based on the results of Appendix A.

Theorem 1: Given the geometry of the probe described by the array of parameters $\mathbf{p}$, the probe liftoff l_0, and the tilting θ of the probe with respect to the plate, the thickness Δ satisfies the following equation:

$$\omega_{\min} \sigma \mu_0 D^2 = h\left(\frac{\Delta}{D}, \frac{l_0}{D}, \theta, \mathbf{p}\right) \tag{5}$$

where D is the size of the probe and $h(\cdot)$ a proper function.

We call (5) the FTE.

Remark 1: The FTE (5) involves function $h(\cdot)$, which can be evaluated numerically. Specifically, given the probe geometry ($\mathbf{p}$ and D), the liftoff l_0, and the tilting θ, function $h(\cdot)$ depends only on thickness Δ, and it may be precomputed and stored.

Remark 2: It is worth noting that the FTE (5) could be derived directly from the Dodd and Deeds analytical representation, but dealing with that analytical representation is somewhat involved. Moreover, the method proposed to derive (5) is completely general, independent of the underlying geometry, and it can be applied without major changes to other geometrical configurations, such as pipes.

Theorem 1 is complemented by the following results concerning the asymptotic behavior for $\Delta/D \to 0^+$ and for $\Delta/D \to +\infty$.

Theorem 2: Given the geometry of the probe described by the array of parameters $\mathbf{p}$, the probe liftoff l_0, and the tilting θ of the probe with respect to the plate, $\omega_{\min}$ satisfies the following relationships:

$$\omega_{\min} \sigma \mu_0 D \Delta \sim h_0\left(\frac{l_0}{D}, \theta, \mathbf{p}\right), \quad \text{for } \Delta/D \to 0^+ \tag{6}$$

$$\omega_{\min} \sigma \mu_0 D^2 \sim h_\infty\left(\frac{l_0}{D}, \theta, \mathbf{p}\right), \quad \text{for } \Delta/D \to +\infty \tag{7}$$

where D is the size of the probe, and $h_0(\cdot)$ and $h_\infty(\cdot)$ are the proper functions.

The proofs of Theorems 1 and 2 are given in Appendix B.

The connection between Theorems 1 and 2 and (2) is obtained by multiplying both sides of (5) by Δ, which gives

$$\Delta = \delta_{\min}^2 \alpha(\Delta) \tag{8}$$

where

$$\alpha(\Delta) = \frac{\Delta}{2D^2} h\left(\frac{\Delta}{D}, \frac{l_0}{D}, \theta, \mathbf{p}\right). \tag{9}$$

Hereafter, for the sake of simplicity, it is understood that $\alpha(\cdot)$ depends on Δ, D, $\mathbf{p}$, l_0, and θ. Equation (8) is simply (5) cast in a form close to (2). It replaces and generalizes (2).

Theorem 2 can be "translated" in terms of the function $\alpha(\cdot)$. Specifically, (6) combined with (8) gives

$$\alpha(\Delta) \sim \frac{1}{2D} h_0\left(\frac{l_0}{D}, \theta, \mathbf{p}\right), \quad \text{for } \Delta/D \to 0^+ \tag{10}$$

and, similarly, (7) gives

$$\alpha(\Delta) \sim \frac{\Delta}{2D^2} h_\infty\left(\frac{l_0}{D}, \theta, \mathbf{p}\right), \quad \text{for } \Delta/D \to +\infty. \tag{11}$$

Equation (10) implies that $\alpha(\Delta)$ approaches a constant limit for small Δ. This proves that (2) corresponds to (8) in the limit for $\Delta \ll D$. Equation (11) implies that $\alpha(\Delta)$ is proportional to Δ, for large Δ.

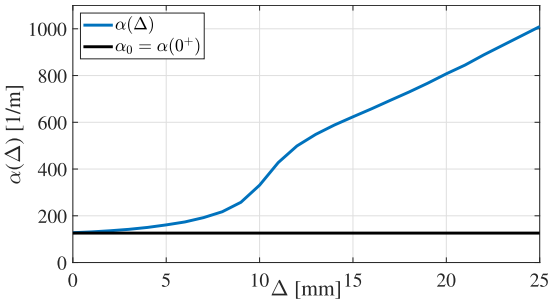

Fig. 2. Complete behavior of $\alpha(\Delta)$ for the probe of Section VI (blue line), together with its constant approximation ($\alpha_0 = 126.28$ m^{-1}) valid for small Δ/D (black line).

Fig. 2 shows the complete behavior of $\alpha(\Delta)$ for a range of thicknesses of interest from 0.01 up to 25 mm, together with its constant approximation for $\Delta \ll D$. It is fairly evident that $\alpha(\cdot)$ cannot be retained constant with respect to the thickness Δ.

Moreover, it is worth noting that $\alpha(\cdot)$ does not depend on the electrical conductivity, as it clearly follows from (9).

Function $\alpha(\cdot)$ represents the "signature" of a given probe for a given liftoff and tilting. To compute it numerically, we express $\alpha(\Delta)$ as

$$\alpha(\Delta) = \frac{\sigma \mu_0 \omega_{\min} \Delta}{2}. \tag{12}$$

Then, we numerically evaluate $\omega_{\min}$ for different values of Δ and/or electrical conductivities σ, and plug these values into (12). In this article, the analysis was carried out numerically, by means of the well-known Dodd and Deeds semianalytical model [24].

Remark 3: It is worth noting that the FTE (5) or (8) allows a clear factorization of the effects due to the geometry and the material. Specifically, $h(\cdot)$ and $\alpha(\cdot)$ account for the geometry of the problem, whereas $\delta_{\min}$ accounts for the material properties (σ and μ_0), other than the angular frequency $\omega_{\min}$ where the minimum is achieved.

Remark 4: Equation (8) can be written as

$$\omega_{\min} = \frac{\alpha(\Delta)}{2\mu_0 \sigma \Delta}. \tag{13}$$

Equation (13), combined with Fig. 2 and the asymptotic behaviors of (10) and (11), shows that $\omega_{\min}$ is inversely proportional to the unknown thickness Δ for $\Delta/D \ll 1$; then, $\omega_{\min}$ decreases with Δ at a decreasing rate until it becomes constant for $\Delta/D \gg 1$. Moreover, if it is known a priori that the unknown thickness is in the range $[\Delta_1, \Delta_2]$, then the proper frequency range for collecting the measurements is $[\omega_1, \omega_2]$, where $\omega_k = \alpha(\Delta_k)/(2\mu_0 \sigma \Delta_k)$.

IV. Intrinsic Limits of the Method: The Critical Thickness

The enhanced equation (8) makes it possible to evaluate the limits of applicability of the proposed method.

To this purpose, we observe that solving (8) entails finding the intersection in the (Δ, α) plane between the straight line $\Delta/\delta^2_{\min}$ and the function $\alpha(\Delta)$.

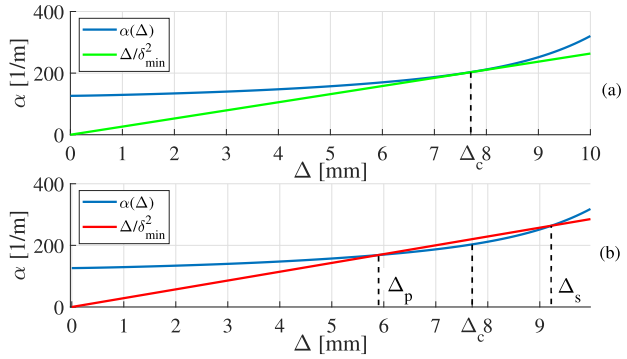

Fig. 3. (a) Geometrical definition of the critical thickness Δ_c. (b) At any higher slope ($\delta_{\min} < \delta_c$) of the straight line, we have only one intersection in the interval $[0, \Delta_c]$.

When the straight line is tangential to the graph of the function $\alpha(\Delta)$ [see Fig. 3(a)], the abscissa of the tangent point defines a thickness value, termed the critical thickness Δ_c, and the skin-depth ($\delta_{\min}$) for the tangent line is termed the critical skin-depth or, in short, δ_c.

In general, (8) admits a solution if and only if the slope of the straight line $\Delta/\delta^2_{\min}$ is higher than that of the tangent line, i.e., if and only if $\delta_{\min} < \delta_c$. In this case, the method gives multiple solutions [Δ_P and Δ_S shown Fig. 3(b)]. However, by restricting the method to the interval $(0, \Delta_c)$, the uniqueness of the solution is restored.

The critical thickness Δ_c is an important parameter because it represents the upper limit of applicability of the method. Δ_c depends on the function $\alpha(\cdot)$, which, in turns, depends on the probe. Δ_c can be used to properly select the probe, according to the range of thicknesses of interest.

Connected to the critical length Δ_c is the concept of critical angular frequency ω_c, which is defined as

$$\omega_c = \frac{\alpha(\Delta_c)}{2\mu_0 \sigma \Delta_c}. \tag{14}$$

The critical angular frequency ω_c represents the smallest angular frequency, where $\Delta R(\omega)/\omega$ may achieve its minimum. This value can be chosen to set the lower limit of the frequency range where the measurements need to be collected.

V. Proposed Approaches

In this section, we propose two algorithms to solve the FTE (8). This procedure has been developed in order to make the approach suitable for an industrial environment, where automated measurements with minimal a priori knowledge of the nominal thickness of the metal plates are required.

Both algorithms are based on a preliminary evaluation of the function $\alpha(\cdot)$ in the range of thicknesses of interest, for the given geometry of the probe, liftoff, and tilting. This preliminary evaluation, made once for all, can be carried out through an experimental, numerical, or mixed procedure (i.e., considering both experimental and numerical points).

The first algorithm to solve (8) is iterative, and the second is analytical.

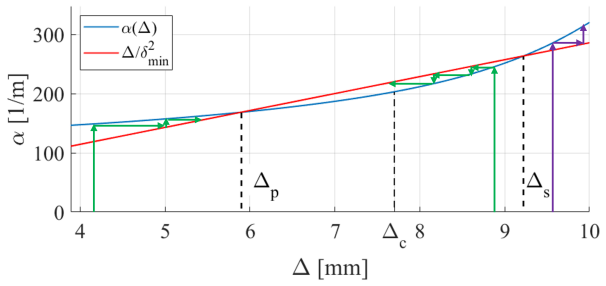

Fig. 4. Evidence of the convergence of the iterative solution. For any initial point smaller than the second roots Δ_s, the algorithm converges to the primary root $\Delta_p < \Delta_c$. After Δ_s, the iterative scheme does not converge. Since the value of Δ_sn is not known, the iteration is initialized with $\Delta_1 < \Delta_c$.

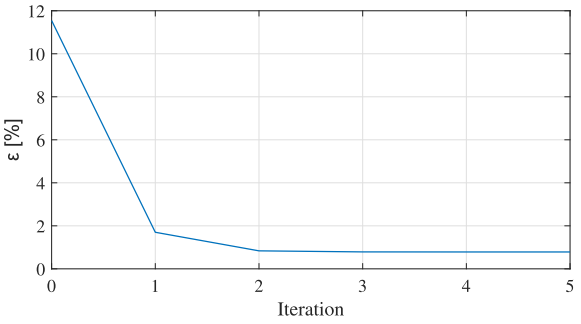

Fig. 5. Plot of the percentage relative error on the estimate of the thickness, as a function of the number of iterations.

A. Iterative Approach

In this section, we propose an iterative approach to obtain the proper value of the unknown thickness Δ, taking into account the FTE (8), where $\alpha(\Delta)$ was introduced. As mentioned above, $\alpha(\cdot)$ is assumed to be available in the range of interest.

The estimated thickness via the iterative method is obtained by the following steps.

1) *Measurement:* Measure $\omega_{\min}$, the angular frequency, where $\Delta R(\omega)/\omega$ achieves its minimum.
2) *Initialization:* Compute $\delta_{\min}$ according to (4), set $i = 1$, and select an arbitrary Δ_1 in the interval $(0, \Delta_c)$.
3) *Update of* Δ*:* Update Δ as
$$\Delta_{(i+1)} = \delta_{\min}^2 \alpha(\Delta_i). \tag{15}$$
4) *Stopping Criterion:* If $|\Delta_{(i+1)} - \Delta_{(i)}| < e$, set $\Delta = \Delta_{(i+1)}$ and exit. Otherwise, set $i = i + 1$ and go to Step 3.

In Step 4, $e > 0$ is an absolute error tolerance used for the stopping criterion.

The algorithm described in Steps 1–4 is simply a fixed-point method to solve the fixed-point equation (8). Moreover, it converges to the proper solution, regardless of the choice of initial point $\Delta_1 \in (0, \Delta_c)$, as shown in Fig. 4 and discussed in Appendix C.

A few iterations are usually required to achieve a proper convergence. For example, considering the test conditions defined in Section III ($\Delta_{\min} = 0.1$ mm and $\Delta_{\max} = 7$ mm) and assuming an unknown thickness of 2 mm and a threshold e equal to 15 μm, Fig. 5 shows that the correct evaluation of the thickness is achieved in three steps only. In particular, starting from an initial error on the thickness estimate of 11.80%, the iterative solution is reduced to 0.78% in just three steps.

In short, including this iterative solution in the proposed ECT-based thickness measurement method enables a considerable improvement in the accuracy of the final thickness measurement for a minimal computational effort. In fact, the time taken by the iterative solution can be considered negligible since it is dependent on only a few accesses to a lookup table/interpolation rule generating the values of $\alpha(\cdot)$.

B. Analytical Approach

In this section, the proposed analytical approach is described. It is based on a polynomial approximation of the function $\alpha(\cdot)$, the latter assumed to be known, as mentioned above. The minimum number of samples of $\alpha(\cdot)$ required to calculate the polynomial coefficients depends on the degree of polynomial approximation.

In analytical terms, we have

$$\alpha(\Delta) \approx \sum_{i=0}^{N} c_i \cdot (\Delta - \Delta_0)^i \tag{16}$$

where c_is are the polynomial coefficients and Δ_0 is the point of expansion of this approximation. When $N = 0$ and $\Delta_0 = 0$, we have the approximation underlying (2) It is worth noting that Approximation (16) makes the FTE (8) an algebraic equation.

The estimated thickness via the analytical method is obtained through the following steps.

1) *Measurement:* Measure $\omega_{\min}$, the angular frequency where $\Delta R(\omega)/\omega$ achieves its minimum.
2) *Initialization:* Compute $\delta_{\min}$ according to (4).
3) *Computation of* Δ*:* Solve
$$\Delta = \delta_{\min}^2 \sum_{i=0}^{N} c_i \cdot (\Delta - \Delta_0)^i. \tag{17}$$

It is worth noting that algebraic equation (17) can be solved in real time with today's computational resources.

A very useful and interesting case is that of $N = 2$. In this case, (17) for $\Delta_0 = 0$ reduces to

$$\frac{\Delta}{\delta_{\min}^2} = c_0 + c_1 \cdot \Delta + c_2 \cdot \Delta^2. \tag{18}$$

The analytical solution of (18) is

$$\Delta = \frac{-\left(c_1 - \delta_{\min}^{-2}\right) - \sqrt{\left(c_1 - \delta_{\min}^{-2}\right)^2 - 4c_0c_2}}{2c_2} \tag{19}$$

where the sign of the square root is chosen to have the physically admissible solution, which is smaller than Δ_c. Moreover, a simple calculation carried out under this second-order approximation gives $\Delta_c = (c_0/c_2)^{1/2}$.

From a general perspective, it is necessary to choose the degree N of the interpolant based on a compromise between the ease in computing the solution of (17) and the residual error in approximation (16). To this purpose, it is useful to

TABLE I

RMSE VALUES OBTAINED WITH THE CONSIDERED THICKNESS RANGE VERSUS DIFFERENT DEGREES OF THE INTERPOLATING POLYNOMIAL

Polynomial degree	RMSE [1/m]
1	3.961
2	0.742
3	0.365
4	0.348
5	0.349
6	0.349

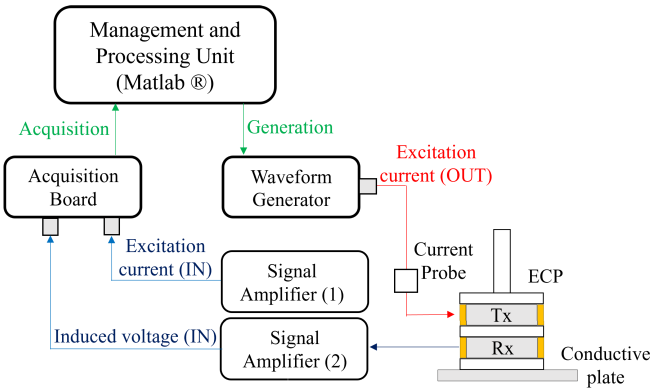

Fig. 6. Block diagram of the adopted measurement setup.

compute the approximation errors in terms of the root-mean-square error (RMSE) defined as

$$\text{RMSE} = \sqrt{\frac{\sum_{i=1}^{K}\left[\hat{\alpha}(\Delta_i) - \alpha(\Delta_i)\right]^2}{K}} \tag{20}$$

where $\hat{\alpha}(\cdot)$ is the approximating polynomial, Δ_i is the ith sampling point, and K is the total number of samples.

Table I reports the RMSE for different values of the order of the polynomial approximation N, for the same case described above. It is worth noting that for $N = 4$ (the fourth-order polynomial), the RMSE reaches its plateau, where the approximation error is not larger than the numerical errors in computing the function $\alpha(\cdot)$. A higher order polynomial would not improve the overall accuracy, despite requiring a higher computational cost.

As a final comment, we highlight that approximation (16) is very interesting when the function $\alpha(\cdot)$ is acquired experimentally. Indeed, the c_is in expansion (16) can be found via a minimum set of $N + 1$ measurements, carried out on plates of known thickness and electrical properties. Moreover, this experimental characterization does not require the exact knowledge of the probe geometry, thus making this approach the only option when the function $\alpha(\cdot)$ cannot be computed numerically because of the lack of knowledge of the probe or uncertain parameters.

VI. EXPERIMENTAL SETUP AND CASE STUDIES

A schematic block diagram of the measurement setup is shown in Fig. 6. The experimental setup comprises the following components: an eddy-current probe (ECP), a waveform generator, a data acquisition board, a current probe, and two

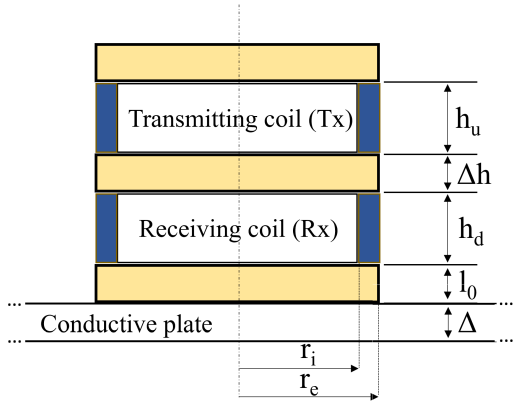

Fig. 7. ECP geometry. The coil windings (blue) together with the plastic holder (yellow).

TABLE II

GEOMETRIC PARAMETERS OF THE ADOPTED ECP

r_i [mm]	11.8
r_e [mm]	12.2
$h_u = h_d$ [mm]	3
Δh (gap) [mm]	1
l_0 (lift-off) [mm]	0.5
$N1 = N2$ (number of turns)	20

TABLE III

CHARACTERISTICS OF THE CONSIDERED CASE STUDIES

Metal alloy	Nominal thickness [mm]	Electrical conductivity [MS/m]	Plate dimensions [cm x cm]
EN AW-1050A (Metallog)	0.469	35.4	13 x 18
	1.035	35.3	25 x 25
	1.969	35.0	25 x 50
	2.912	35.3	25 x 25
	3.994	34.5	25 x 25
2024T3 (Casoni)	2.003	18.8	20 x 20

signal amplifiers. The ECP consists of two coaxial coils, the upper coil used as the transmitting coil (Tx) and the lower coil as the receiving coil (Rx). The coils' geometry is shown in detail in Fig. 7; their dimensions are given in Table II. A Waveform Generator Agilent 33120A is used to provide the excitation current to the Tx. The excitation current has been sensed by means of a current probe Tektronix TCP202A, and both the sensed excitation current and the induced voltage on the receiving coil Rx were conditioned using two SR560 Stanford Research System low-noise amplifiers, which amplify and filter the signals. An Acquisition board TIE-PIE Engineering Handyscope HS5-540XMS-W5(TM) is used to acquire both the conditioned signals with a sampling frequency of 1000 times the frequency of the exciting signal and 14 bits of resolution. The tests were carried out by feeding the exciting coil with a sinusoidal frequency-swept signal. The range of frequencies of interest was from 200 to 3 kHz, with a resolution of 2 Hz and with a root mean square current value of 135 mA. The Management and Processing unit includes an MATLAB algorithm running on a dual-core PC for processing

TABLE IV
COMPARISON BETWEEN THE THICKNESSES OBTAINED BY USING THE TRUE VALUE OF $\alpha(\Delta)$, THE α_0 VALUE REFERRED TO Δ_{REF}, AND THE TWO PROPOSED SOLUTIONS

Actual thickness [mm]	**(a) Solution via the thought experiment**		**(b) Solution via the approach of [10]**		**(c) Solution via the iterative method**		**(d) Solution via the analytical method (second-degree)**		**(e) Solution via the analytical method (fourth-degree)**	
	Estimated thickness [mm]	RTE [%]	Estimated thickness [mm]	RTE [%]	Estimated thickness [mm]	RTE [%]	Estimated thickness [mm]	RTE [%]	Estimated thickness [mm]	RTE [%]
0.469	0.463	1.35	0.453	3.50	0.463	1.35	0.465	0.85	0.463	1.35
1.035	1.041	0.61	1.007	2.68	1.047	1.16	1.046	1.13	1.047	1.16
1.969	1.952	0.86	1.813	7.91	1.949	1.02	1.937	1.60	1.948	1.06
2.003	2.006	0.16	1.863	6.97	2.007	0.19	1.995	0.38	2.007	0.19
2.912	2.901	0.38	2.588	11.12	2.899	0.43	2.886	0.89	2.902	0.36
3.994	4.001	0.18	3.416	14.48	4.073	1.96	4.091	2.43	4.084	2.24

the acquired data, managing both the waveform generator and the acquisition board TIE-PIE.

The experimental tests were carried out considering six reference aluminum plates, whose nominal thickness values, electrical conductivities, and dimensions are given in Table III. A 2024T3 aluminum plate with a thickness of 2.003 mm and five EN AW-1050A aluminum plates with different thicknesses from 0.5 to 4 mm have been considered in this study.

VII. EXPERIMENTAL RESULTS

In this section, the experimental results achieved by using the proposed approach are presented and discussed.

The experimental campaign was carried out using the measurement setup, the sample plates, and the frequency-swept excitation described in Section VI. The aim was to analyze the accuracy of the proposed methods based on the FTE (8).

The experimental results have been organized in terms of comparison between the following strategies.

(1) estimating Δ assuming the a priori knowledge of $\alpha(\cdot)$, evaluated at Δ.
(2) estimating Δ through the approach of [10].
(3) estimating Δ through the iterative approach with $e = 15\ \mu$ m.
(4) estimating Δ through the analytical approach with a second-degree polynomial.
(5) estimating Δ through the analytical approach with a fourth-degree polynomial.

Approach 1) corresponds to a thought experiment since it requires the knowledge of $\alpha(\cdot)$ at the unknown thickness value, which is not available in a practical setting. However, this approach gives the best accuracy that can be achieved. Indeed, the errors are only due to the uncertainty in the experimental setup and to the accuracy in computing $\alpha(\cdot)$. The value of Δ used in evaluating function $\alpha(\cdot)$ at the right-hand side of (8) is that of the nominal thickness shown in Table III.

Thickness estimation performance has been compared in terms of the relative thickness error (RTE), defined as

$$\text{RTE} = \frac{\Delta_e - \Delta_a}{\Delta_a} \cdot 100 \tag{21}$$

where Δ_a is the actual thickness of the sample and Δ_e is the estimated thickness. Table IV summarizes the obtained experimental results for the configurations of Table III.

As expected, the smallest RTEs were observed by adopting approach 1), with RTEs lower than 1% except for the sample with a thickness of 0.469 mm, for which an RTE of 1.35% was found. For the original approach of [10], based on (2), the RTE significantly worsened, rising to 14%. The smallest error (2.68%) is obtained for a thickness equal to 1 mm. The new approaches of Section V, namely 3)-5), yield an excellent performance. Indeed, the RTEs are always lower than 2.5% and, in several cases, are comparable with the "ideal" values obtained by using the a priori knowledge of $\alpha(\cdot)$, i.e., the thought experiment.

VIII. CONCLUSION

This article proposes a novel measurement method for the estimation of the thickness of the metallic plates. The method is specifically designed for accurate, online, and real-time applications.

The theory underlying the proposed method explains the transfer characteristic, i.e., the relationship between the measured quantity $\omega_{\min}$ and the unknown thickness Δ, for arbitrary thicknesses $0 < \Delta < +\infty$. This theory has been derived with an entirely new approach based on the celebrated Buckingham π theorem, here applied for the very first time in the framework of nondestructive testing. A strength of the proposed approach based on the Buckingham π theorem is that it can be easily extended to other geometries, different from the planar ones.

The complete knowledge of the transfer characteristic made it possible to find the physical limit of the probe, namely, the critical thickness Δ_c: the measurement of any thickness smaller than Δ_c can be carried out safely, i.e., the solution of the FTE (8) exists, is unique, and depends continuously on the data.

Complementary to the theory, this contribution proposes two algorithms for estimating the unknown thickness. The first approach is based on an iterative method (fixed point method) for which a proof of its convergence has been provided. The second approach is an analytical method, where the thickness is found as the solution of an algebraic equation, and is based on a local (polynomial) approximation of function $\alpha(\cdot)$. From a general perspective, the iterative approach may be preferred for applications where the probe is used on the full range, from 0 to the critical thickness Δ_c, whereas the analytical approach may be preferred when the target thicknesses vary in a local neighborhood where the polynomial approximation can be made accurate with only a few terms.

The experimental results confirmed the accuracy of the proposed approaches, with relative errors lower than 2.5%, and comparable with the ideal ones, that can be obtained in a thought experiment exploiting the knowledge of the "unknown" thickness.

Finally, future work will comprise the extension of the Buckingham π theorem to structures made by multiple layers or problems where the liftoff is uncertain.

APPENDIX

A. Dimensional Analysis

In this Appendix, we derive the functional relationships between $\Delta\dot{Z} = \dot{Z}_m^A - \dot{Z}_m^P$ and the problem parameters.

The starting point is that $\Delta\dot{Z}$ depends on the following quantities.

1) the angular frequency of the excitation signal ω.
2) the physical properties of the plate σ and μ_0.
3) the thickness of the plate Δ.
4) the normalized geometry of the probe $\mathbf{p}$.
5) the overall size of the probe D.
6) the liftoff l_0 and the tilting θ.

Here, D is a length giving the overall size of the probe and $\mathbf{p}$ is a vector containing all the geometric parameters of the probe, but where lengths are normalized to probe size D. In our case (see Table II), we have

$$\mathbf{p} = \left[\frac{r_i}{D}, \frac{r_e}{D}, \frac{h_u}{D}, \frac{h_d}{D}, \frac{\Delta h}{D}, N_1, N_2\right]. \tag{22}$$

Parameter D can be chosen arbitrarily, as long as it represents the linear size of the probe. For instance, D can be chosen as the external diameter of the coils, i.e., $D = 2r_e$. Finally, l_0 and θ are the distance and the inclination of the probe to the plate, respectively.

In mathematical terms, we have

$$\Delta\dot{Z} = \dot{Z}_m^A - \dot{Z}_m^P = g(\omega, \sigma, \mu_0, \Delta, l_0, \theta, D, \mathbf{p}) \tag{23}$$

where g is a proper complex function.

To analyze the "essential" dependencies among the variables involved in (23), we use the celebrated Buckingham π theorem [25]. The latter formalizes the concept that the laws of physics are independent of the measurement units. These fundamental results in the field of dimensional analysis have been successfully used in various areas such as [26], [27], [28], and [29]. To the best of our knowledge, this is the first application of dimensional analysis in the framework of NDT.

In order to apply the Buckingham π theorem, it is necessary to choose: 1) the fundamental dimensions and 2) the repeating variables (see [25] for definitions and details). In our case, length, time, and impedance were chosen as fundamental dimensions, and μ_0, ω, and D as repeating variables. Then, the Buckingham π theorem allows (23) to be cast in a dimensionless form as

$$\frac{\Delta\dot{Z}}{\omega\mu_0 D} = f\left(\omega\sigma\mu_0 D^2, \frac{\Delta}{D}, \frac{l_0}{D}, \theta, \mathbf{p}\right) \tag{24}$$

where f is a proper function.

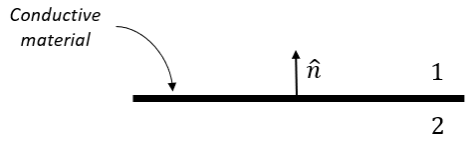

Fig. 8. Plate for small Δ, together with the orientation of the normal vector and the definition of regions 1 and 2.

With a similar approach, the Buckingham π theorem makes it possible to find the limiting behavior of (24) for $\Delta \ll D$. Indeed, in this case (thin shell limit), the conducting material behaves as a planar surface S where the following jump condition holds (see Fig. 8):

$$\hat{\mathbf{n}} \times (\mathbf{H}_1 - \mathbf{H}_2) = \sigma\Delta(\hat{\mathbf{n}} \times \mathbf{E}) \times \hat{\mathbf{n}}, \quad \text{on } S. \tag{25}$$

This implies that, for small Δ, the electromagnetic field depends on the $\sigma\Delta$ product, rather than on σ and Δ separately. Therefore, (23) is replaced by

$$\Delta\dot{Z} \sim g_0(\omega, \sigma\Delta, \mu_0, l_0, \theta, D, \mathbf{p}) \tag{26}$$

which, in dimensionless form, can be cast as

$$\frac{\Delta\dot{Z}}{\omega\mu_0 D} \sim f_0\left(\omega\mu_0 D\sigma\Delta, \frac{l_0}{D}, \theta, \mathbf{p}\right) \tag{27}$$

where both g_0 and f_0 are proper functions.

To complete the analysis, we discuss the case $\Delta \gg D$. In this case, $\Delta\dot{Z}$ does not depend on Δ, because the probe is "unable" to interact with the bottom of the plate. Therefore, (24) can be replaced by

$$\frac{\Delta\dot{Z}}{\omega\mu_0 D} \sim f_\infty\left(\omega\sigma\mu_0 D^2, \frac{l_0}{D}, \theta, \mathbf{p}\right) \tag{28}$$

where f_∞ is the limit of f for $\Delta/D \to +\infty$.

B. Proofs of Theorems 1 and 2

Proof: The starting point is the dimensionless equation (24) for $\Delta\dot{Z}$ derived in Appendix A. Specifically, its real part gives

$$\frac{\Delta R}{\omega\mu_0 D} = f_R\left(\omega\sigma\mu_0 D^2, \frac{\Delta}{D}, \frac{l_0}{D}, \theta, \mathbf{p}\right) \tag{29}$$

where $f_R(\cdot) = \mathrm{Re}\{f(\cdot)\}$.

When the left-hand side of (29) achieves its minimum, we have

$$\frac{\partial f_R}{\partial a_1}\left(\omega_{\min}\sigma\mu_0 D^2, \frac{\Delta}{D}, \frac{l_0}{D}, \theta, \mathbf{p}\right) = 0 \tag{30}$$

where $\partial/\partial a_1$ represents the partial derivative with respect to the first argument of the function f_R.

Assuming that (30) can be solved with respect to its first argument, (5) follows, where $h(\cdot)$ is a proper function. □

Proof: The proof of (6) and (7) follows that of Theorem 1, but starting from (27) and (28), respectively. □

C. Convergence of the Iterative Method

To prove this result, we first observe that solving (8) for Δ corresponds to solving a fixed-point problem, i.e., a problem of the type

$$\Delta = f(\Delta \tag{31}$$

for $f(\Delta) = \delta_{\min}^2 \alpha(\Delta)$.

Then, the iterative method of Section V-A is convergent because: 1) the function $f(\cdot)$ is a contraction[1] and 2) the interval $[0, \Delta^*]$ with $\Delta^* < \Delta_c$ is a complete metric space. Indeed, under these two conditions, we can invoke the Banach fixed-point theorem [30], which guarantees the existence and uniqueness of the solution Δ of (31) and provides a constructive method to find Δ as the limit for $n \to +\infty$ of the sequence $\Delta_{n+1} = f(\Delta_n)$ for $n \in \mathbb{N}$, being $\Delta_1 \in [0, \Delta^*]$.

Since condition 2) is well known, here, we prove condition 1) only. Specifically, we have the following Proposition.

Proposition 1: $f(\cdot)$ is a contraction in $[0, \Delta^*]$, where $0 < \Delta^* < \Delta_c$.

Proof: A sufficient condition for $f(\cdot)$ to be a contraction is proving that its first derivative is smaller than unity in the reference interval $[0, \Delta^*]$.

In our case, we notice that (see Fig. 3) α' is monotonically increasing and, that, $\alpha'(\Delta_c) = 1/\delta_{\min}^2$. Therefore, $\alpha'(x) \leq \alpha'(\Delta^*) < 1/\delta_{\min}^2$ for $x \leq \Delta^* < \Delta_c$. Consequently, $0 \leq f'(x) \leq f'(\Delta^*) < 1$. □

REFERENCES

[1] G. Betta, L. Ferrigno, M. Laracca, A. Rasile, and A. Sardellitti, "Thickness measurements with eddy current and ultrasonic techniques," in *Sensors and Microsystems*, G. E. A. Di Francia, Ed. Cham, Switzerland: Springer, 2020, pp. 387–394.

[2] Z. Zhang et al., "A new laser displacement sensor based on triangulation for gauge real-time measurement," *Opt. Laser Technol.*, vol. 40, no. 2, pp. 252–255, 2008.

[3] A. Bastas, "Comparing the probing systems of coordinate measurement machine: Scanning probe versus touch-trigger probe," *Measurement*, vol. 156, May 2020, Art. no. 107604.

[4] L. Wang and R. X. Gao, *Condition Monitoring and Control for Intelligent Manufacturing*. Cham, Switzerland: Springer, 2006, pp. 1–6.

[5] K.-M. Lee, C.-Y. Lin, B. Hao, and M. Li, "Coupled parametric effects on magnetic fields of eddy-current induced in non-ferrous metal plate for simultaneous estimation of geometrical parameters and electrical conductivity," *IEEE Trans. Magn.*, vol. 53, no. 10, pp. 1–9, Oct. 2017.

[6] M. Lu et al., "Thickness measurement of non-magnetic steel plates using a novel planar triple-coil sensor," *NDT & E Int.*, vol. 107, Oct. 2019, Art. no. 102148. [Online]. Available: https://www.sciencedirect.com/science/article/pii/S0963869519302221

[7] J. García-Martín, J. Gómez-Gil, and E. Vázquez-Sánchez, "Non-destructive techniques based on eddy current testing," *Sensors*, vol. 11, no. 3, pp. 2525–2565, Feb. 2011. [Online]. Available: https://www.mdpi.com/1424-8220/11/3/2525

[8] E. Pinotti and E. Puppin, "Simple lock-in technique for thickness measurement of metallic plates," *IEEE Trans. Instrum. Meas.*, vol. 63, no. 2, pp. 479–484, Feb. 2013.

[9] W. Cheng, "Thickness measurement of metal plates using swept-frequency eddy current testing and impedance normalization," *IEEE Sensors J.*, vol. 17, no. 14, pp. 4558–4569, Jul. 2017.

[10] W. Yin and A. J. Peyton, "Thickness measurement of non-magnetic plates using multi-frequency eddy current sensors," *NDT & E Int.*, vol. 40, no. 1, pp. 43–48, Jan. 2007.

[11] A. Sardellitti, G. D. Capua, M. Laracca, A. Tamburrino, S. Ventre, and L. Ferrigno, "A fast ECT measurement method for the thickness of metallic plates," *IEEE Trans. Instrum. Meas.*, vol. 71, pp. 1–12, 2022.

[12] W. Yin and K. Xu, "A novel triple-coil electromagnetic sensor for thickness measurement immune to lift-off variations," *IEEE Trans. Instrum. Meas.*, vol. 65, no. 1, pp. 164–169, Jan. 2016.

[13] M. Lu, L. Yin, A. J. Peyton, and W. Yin, "A novel compensation algorithm for thickness measurement immune to lift-off variations using eddy current method," *IEEE Trans. Instrum. Meas.*, vol. 65, no. 12, pp. 2773–2779, Aug. 2016.

[14] M. Fan, B. Cao, A. I. Sunny, W. Li, G. Tian, and B. Ye, "Pulsed eddy current thickness measurement using phase features immune to liftoff effect," *NDT & E Int.*, vol. 86, no. 3, pp. 123–131, 2017.

[15] H. Wang, J. Huang, L. Liu, S. Qin, and Z. Fu, "A novel pulsed eddy current criterion for non-ferromagnetic metal thickness quantifications under large liftoff," *Sensors*, vol. 22, no. 2, p. 614, Jan. 2022. [Online]. Available: https://www.mdpi.com/1424-8220/22/2/614

[16] N. Ulapane, K. Thiyagarajan, J. V. Miro, and S. Kodagoda, "Surface representation of pulsed eddy current sensor signals for improved ferromagnetic material thickness quantification," *IEEE Sensors J.*, vol. 21, no. 4, pp. 5413–5422, Feb. 2021.

[17] D. G. Park, C. S. Angani, G. D. Kim, C. G. Kim, and Y. M. Cheong, "Evaluation of pulsed eddy current response and detection of the thickness variation in the stainless steel," *IEEE Trans. Magn.*, vol. 45, no. 10, pp. 3893–3896, Oct. 2009.

[18] J. Ge, N. Yusa, and M. Fan, "Frequency component mixing of pulsed or multi-frequency eddy current testing for nonferromagnetic plate thickness measurement using a multi-gene genetic programming algorithm," *NDT & E Int.*, vol. 120, Jun. 2021, Art. no. 102423. [Online]. Available: https://www.sciencedirect.com/science/article/pii/S0963869521000220

[19] *En 485-4:2000*. Accessed: Jul. 4, 2022. [Online]. Available: https://infostore.saiglobal.com/en-gb/standards/ds-en-485-4-2000-462686_saig_ds_ds_1042214/

[20] M. Lu, Y. Xie, W. Zhu, A. J. Peyton, and W. Yin, "Determination of the magnetic permeability, electrical conductivity, and thickness of ferrite metallic plates using a multifrequency electromagnetic sensing system," *IEEE Trans. Ind. Informat.*, vol. 15, no. 7, pp. 4111–4119, Jul. 2019.

[21] A. Bernieri, G. Betta, L. Ferrigno, and M. Laracca, "Improving performance of GMR sensors," *IEEE Sensors J.*, vol. 13, no. 11, pp. 4513–4521, Nov. 2013.

[22] C. Ye, Y. Wang, M. Wang, L. Udpa, and S. S. Udpa, "Frequency domain analysis of magnetic field images obtained using TMR array sensors for subsurface defect detection and quantification," *NDT & E Int.*, vol. 116, Jan. 2020, Art. no. 102284. [Online]. Available: https://www.sciencedirect.com/science/article/pii/S0963869519306632

[23] G. Yang, G. Dib, L. Udpa, A. Tamburrino, and S. S. Udpa, "Rotating field EC-GMR sensor for crack detection at fastener site in layered structures," *IEEE Sensors J.*, vol. 15, no. 1, pp. 463–470, Jan. 2014.

[24] C. V. Dodd and W. E. Deeds, "Analytical solutions to eddy-current probe-coil problems," *J. Appl. Phys.*, vol. 39, no. 6, pp. 2829–2838, May 1968.

[25] E. Buckingham, "On physically similar systems; illustrations of the use of dimensional equations," *Phys. Rev.*, vol. 4, no. 4, pp. 345–376, 1914, doi: 10.1103/PhysRev.4.345.

[26] C. Giuseppina, D. Antonino, and L. Valerio, "Evaluation of building heating loads with dimensional analysis: Application of the Buckingham π theorem," *Energy Buildings*, vol. 154, pp. 479–490, Jan. 2017. [Online]. Available: https://www.sciencedirect.com/science/article/pii/S0378778817318157

[27] R. C. O. Tang et al., "Review on design factors of microbial fuel cells using Buckingham's Pi theorem," *Renew. Sustain. Energy Rev.*, vol. 130, Sep. 2020, Art. no. 109878. [Online]. Available: https://www.sciencedirect.com/science/article/pii/S1364032120301714

[28] L. Rendón-Castrillón, M. Ramírez-Carmona, C. Ocampo-López, and L. Gómez-Arroyave, "Mathematical model for scaling up bioprocesses using experiment design combined with Buckingham Pi theorem," *Appl. Sci.*, vol. 11, no. 23, p. 11338, 2021. [Online]. Available: https://www.mdpi.com/2076-3417/11/23/11338

[29] L. García-Barrachina and A. J. Gámez, "Dimensional analysis of superplastic processes with the Buckingham π theorem," *Metals*, vol. 10, no. 12, p. 1575, Nov. 2020. [Online]. Available: https://www.mdpi.com/2075-4701/10/12/1575

[30] S. Banach, "Sur les opérations dans les ensembles abstraits et leur application aux équations intégrales," *Fundamenta Mathematicae*, vol. 3, pp. 133–181, Jan. 1922.

[1] A function $f(\cdot)$ is termed contraction if $|f(\Delta_a) - f(\Delta_b)| \leq M\,|\Delta_a - \Delta_b|$ with $M < 1$ and for any $\Delta_a, \Delta_b \in [0, \Delta^*]$.

Alessandro Sardellitti (Graduate Student Member, IEEE) was born in Sora, Frosinone, Italy, in 1993. He received the M.S. degree (cum laude) in electrical engineering from the University of Cassino and Southern Lazio, Cassino, Italy, in 2018, where he is currently pursuing the Ph.D. degree in electrical engineering with the Department of Electrical and Information Engineering.

His current research interests include concern to the development of methodologies, numerical models, and measurement set-up suitable for the realization of non-destructive testing (NDT). On such topic, he is authored and coauthored papers published in international journals and conferences.

Filippo Milano (Member, IEEE) received the M.S. degree (summa cum laude) in electrical engineering and the Ph.D. degree in methods, models and technologies for engineering from the University of Cassino and Southern Lazio, Cassino, Italy, in 2018 and 2021, respectively.

He is currently a Research Fellow with the Department of Electrical and Information Engineering, University of Cassino and Southern Lazio. His research interests include the design, implementation and characterization of positioning systems for biomedical and industrial applications, and the development of models and techniques for the predictive batteries diagnosis and thicknesses estimation of metal laminates using eddy-current techniques.

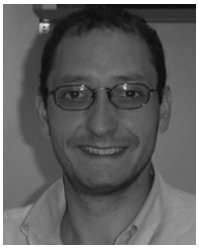

Marco Laracca (Member, IEEE) received the M.S. degree in electrical engineering and the Ph.D. degree in electrical and information engineering from the University of Cassino, Cassino, Italy, in 2002 and 2006, respectively.

From 2006 to 2021, he was an Assistant Professor of electrical and electronic measurements with the University of Cassino, Cassino, Italy. Since 2021, he has been an Associate Professor of electrical and electronic measurements with the Sapienza University of Rome, Rome, Italy. He has been the Chief of the ACCREDIA Notified Metrology Laboratory (LAT 105), since 2018. His current research interests include the realization of the measurement system for nondestructive testing, sensor realization and characterization, electric measurement under nonsinusoidal conditions, and speed calibration.

Salvatore Ventre (Senior Member, IEEE) received the Laurea degree (summa cum laude) in electronic engineering from the University of Naples Federico II, Naples, Italy, in 1990.

Since 1993, he has been with the Department of Electrical and Informational Engineering, University of Cassino and Southern Lazio, Cassino, Italy, where he is currently an Associate Professor of electrotechnics. He has authored or coauthored more than 150 technical papers in international journals and conference proceedings. His current research interests include computational electromagnetic with application in several fields, such as electromagnetic nondestructive evaluation, electromagnetic compatibility, analysis of the time evolution of MHD equilibria, and for the identification of the plasma boundary in tokamaks.

Luigi Ferrigno (Senior Member, IEEE) has been a Full Professor of electric and electronic measurement and the Scientific Manager of the Industrial Measurements Laboratory, University of Cassino, Cassino, Italy, since 2004. In 2008, he was a Founding Member of the University spin-off, Spring Off (University of Salerno), Fisciano, Italy. He is an NDE4.0 Ambassador for the Italian Association of Non-Destructive Evaluation and Test (AiPnD) in the EFNDT WG10. He coordinated and participated in several national and international research projects. His current research interests include the NDT4.0, novel learning sensors and measurement systems for smart city, the Internet of Things (IoT), automotive, smart energy, and environment.

Antonello Tamburrino (Senior Member, IEEE) received the Laurea degree (summa cum laude) in electronic engineering from the University of Naples Federico II, Naples, Italy, in 1992, and the Ph.D. degree in electronic engineering from the Polytechnic of Turin, Turin, Italy, in 1996.

Since 2006, he has been a Full Professor of electrical engineering with the Department of Electrical and Information Engineering, University of Cassino and Southern Latium, Cassino, Italy. Since 2014, he has been a Full Professor of electrical engineering with the College of Engineering, Michigan State University, East Lansing, MI, USA. He has authored or coauthored over 200 papers that have appeared in refereed international journals, books, and proceedings of international conferences, and is a Coeditor of three proceedings. His current research interests include computational electromagnetism, plasmonics, inverse problems, electromagnetic imaging, and nondestructive evaluation of structures and materials.

Dr. Tamburrino is a member of the Scientific Board of the *Journal Nondestructive Testing* and currently a Subject Editor of the scientific journal *NDT and E International*.

Open Access funding provided by 'Università degli Studi di Cassino e del Lazio Meridionale' within the CRUI CARE Agreement